Penetration Depth of Transverse Spin Current in Ultrathin Ferromagnets

A. Ghosh,[1] S. Auffret,[1] U. Ebels,[1] and W. E. Bailey[1,2,*]

[1]*SPINTEC, UMR(8191) CEA/CNRS/UJF/Grenoble INP, INAC, 17 rue des Martyrs, 38054 Grenoble Cedex, France*
[2]*Department of Applied Physics and Applied Mathematics, Columbia University, New York, New York 10027, USA*

We report a novel depth dependence for the penetration of spin current into ultrathin ferromagnets. Ferromagnetic resonance measurements show that transverse spin current pumped into three structurally distinct ferromagnets is attenuated, on reflection, by an amount proportional to the ferromagnetic layer thickness, saturating abruptly at 1.2 ± 0.1 nm. The observed power-law decay, differing significantly from the (exponential) characteristic-length dependence for longitudinal spin current, confirms models of spin momentum transfer which have been inaccessible to experiment.

PACS numbers: 75.47.−m, 76.50.+g, 75.76.+j, 75.78.−n

In spin momentum transfer (SMT) [1,2], a spin-polarized current, injected into a ferromagnetic layer (F), transfers its angular momentum to the F magnetization $\boldsymbol{M}$ as it is absorbed. The depth dependence of spin current absorption in the F is of fundamental interest for SMT. Since injected spins polarized transverse to $\boldsymbol{M}$ are absorbed and exert torque [3,4], the penetration depth has been framed in terms of the transverse spin coherence length λ_c in the F [5–7]. This SMT length scale is thought to be very short, $\lambda_c \leq 2$ nm in $3d$ metallic ferromagnets. Experiments have not probed the dependence of SMT on the several-angstrom scale in the relevant thickness range $t_F < 2$ nm; coarser-resolution experiments performed on thicker Co layers [8,9] include the possibility of some variation in SMT efficiency.

The spin pumping effect [10–12] provides an alternative prospect to study the length scale of SMT. In a spin-valve structure ($F_1/N/F_2$), precession of F_1 sources ("pumps") a spin current across the N and into F_2, where it is absorbed identically to spin-polarized electrical current injected through voltage, verified as torque on the magnetization [13]. Spin pumping can be regarded as an inverse process to current-pumped precession [14,15]: Onsager relations link interfacial spin torque and spin pumping coefficients within a constant of proportionality [16,17]

The real part of the spin mixing conductance $g_r^{\uparrow\downarrow}$ contributes an interfacial Gilbert damping in $F_1/N/F_2$ trilayers [12,18]. This quantity, which is proportional to the Slonczewski spin torque coefficient for a N/F interface, can be accessed conveniently through ferromagnetic resonance (FMR) measurements of extended thin-film stacks. Because these measurements do not require device nanofabrication, they are rapid compared with SMT device measurement for a given film configuration, allowing a larger number of layers to be characterized in finite time. Finite-size magnetostatic [19] and activation volume [9] effects do not enter in the measurement, facilitating interpretation. Moreover, because the Gilbert damping of (thicker) F_i depends on the properties of the (ultrathin)

near-N interface F_j, spin current absorption in layers only a few angstroms thick can be measured as a perturbation on an otherwise robust signal.

Prior magnetotransport measurements have indicated the existence of a *characteristic length* for spin current absorption near the Fermi energy in $3d$ ferromagnets. Giant magnetoresistance measurements [20–22] reveal an exponential decrease of spin polarized current density with increasing depth z in the ferromagnet as $\exp(-z/\lambda_{\mathrm{SD}})$ where λ_{SD} is the spin diffusion length. These measurements refer to the longitudinal component of spin, parallel and antiparallel to $\boldsymbol{M}$. The exponential depth dependence reflects a Poisson process for spin relaxation: spin-flip scattering events are uncorrelated over distance with uniform probability distribution over depth.

A different depth dependence of absorption has been predicted for transverse spin currents in F layers. The length scale is set by the transverse spin coherence length, given to first order by $\lambda_J \sim \pi/|k_f^{\uparrow} - k_f^{\downarrow}|$ where $k_f^{\uparrow(\downarrow)}$ are the majority (minority) Fermi wave vectors [7], or equivalently $\sim h v_g/2\Delta_{\mathrm{ex}}$, with v_g as the spin-averaged group velocity and Δ_{ex} the exchange splitting [23]. This quantity is estimated at 1–2 nm near the Fermi energy in $3d$ ferromagnets [6]. The functional form predicted for total transverse spin current absorption approximates an algebraically decaying sinusoid about a step function [24], with differences depending upon the Fermi surface integration [6,7,24–26]. Experimental results in the regime $t \lesssim \lambda_J$ exist only for hot electrons $E - E_F \geq 5$ eV, injected and detected from vacuum using Mott polarimetry [23,27].

In this Letter, we have measured the depth-dependence of transverse spin current absorption in three ultrathin ferromagnets and one antiferromagnet at E_F using the spin pumping effect. Spin mixing conductances in thicker polycrystalline structures are shown, for the first time, to be in quantitative agreement with theory. In ultrathin films, we observe transverse spin current absorption proportional to thickness with abrupt saturation at a critical depth $\lambda_c = 1.2 \pm 0.1$ nm in the structurally diverse ferromagnets
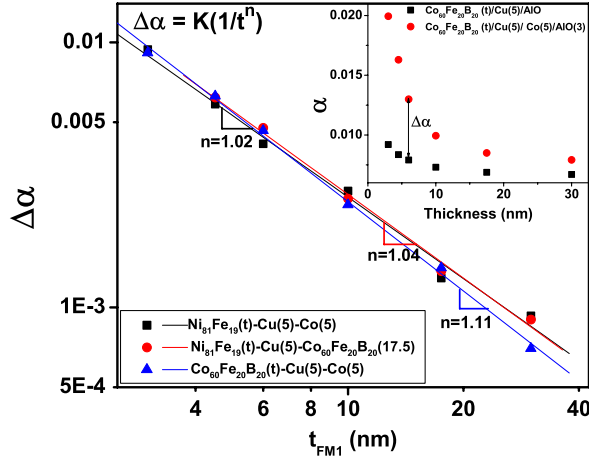
FIG. 1 (color online).   Contributed Gilbert damping $\Delta\alpha(t_{F1}) = \alpha_{F2}(t_{F1}) - \alpha_{\text{no}F2}(t_{F1})$ from the introduction of a second F_2 interface in $\boldsymbol{F_1(t_{F_1})}$/Cu(5 nm)[/$\boldsymbol{F_2}$]/Al(3 nm) structures. Inset: $\alpha_{\text{no}F2}(t_{F1})$ and $\alpha_{F2}(t_{F1})$ for CoFeB layers.
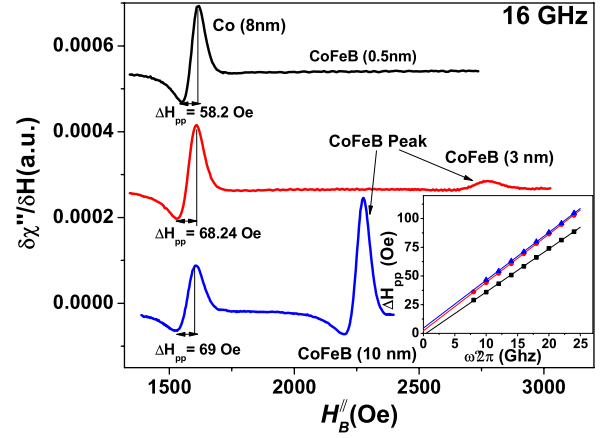

FIG. 2 (color online). Isolation of contribution to Gilbert damping in F_1/Cu/$F_2(t_{F2})$, $F_1 = \text{Co}(8\,\text{nm})$, $F_2 = \text{CoFeB}\,t_{\text{CoFeB}}$. Main panel: Derivative FMR spectra, 16 GHz, $t_{\text{CoFeB}} = 0.5$, 3.0, and 10.0 nm. Note the increase in linewidth for the Co resonance (low field) as a function of t_{CoFeB}. Inset: Separation of intrinsic and extrinsic damping for different t_{CoFeB}.

$\text{Ni}_{81}\text{Fe}_{19}$ ("Py"), $\text{Co}_{60}\text{Fe}_{20}\text{B}_{20}$ ("CoFeB"), and pure Co. Identical behavior is seen in the antiferromagnet $\text{Ir}_{80}\text{Mn}_{20}$, with slightly higher $\lambda_C = 1.5 \pm 0.1$ nm. The observed behavior is highly reminiscent of the spin-polarized hot-electron reflection in Ref [27]. Our measurements are inconsistent with earlier experimental reports of an exponential onset of spin current absorption in F layers [28], and highlight the correlated, path-dependent nature of transverse spin-current absorption predicted by theory.

Layers have been prepared by sputtering on ion-cleaned Si/SiO_2 substrates, seeded in every case with Ta(5 nm)/Cu(5 nm) bilayers, capped in every case with 3 nm Al layers, oxidized in air. All samples have been characterized by variable-frequency (2–24 GHz), swept-field FMR at room temperature. Care has been taken in the deposited sample series to isolate the effect of these covering layers alone, and the frequency range considered has facilitated our isolation of the Gilbert damping constant α in the measurements, as in prior work [29].

First, we show data which support the existence of the spin pumping effect in our $F_1/N/F_2$ heterostructures with the three different F layers considered. Three series of $F_1(t_{F1})$/Cu(5 nm)/F_2/Al(3 nm) structures were prepared for $t_{F_1} = 3, 4.5, 6.0, 10.0, 17.5, 30.0$ nm with and without the F_2 overlayer, with F_1/F_2 combinations Py/Co, Py/CoFeB, CoFeB/Co, for a total of 36 samples. The choices of $t_{F_2} = 5$ nm (Co) and 17.5 nm (CoFeB) avoid overlap of the $F_{1,2}$ resonances.

For each sample, the Gilbert damping α of F_1 has been extracted from the frequency-dependent linewidths $\Delta H(\omega)$ in swept-field FMR measurement. The (intrinsic) Gilbert damping α is isolated from the inhomogeneous broadening ΔH_0 through $\Delta H(\omega) = \Delta H_0 + (2/\sqrt{3})\alpha\omega/\gamma$; see, e.g., Refs [10,29], and Fig. 2, inset, for an example. ΔH measures the width between inflection points in a Lorenzian

absorption line, which appear as maxima in the experimental derivative (lock-in) signal $\partial\chi''/\partial H$ (peak-to-peak linewidth). The offset term ΔH_0 is attributed to inhomogeneities in the local resonance field. The difference $\Delta\alpha(t_{F1}) = \alpha_{F2}(t_{F1}) - \alpha_{\text{no}F2}(t_{F1})$ isolates the effect on Gilbert-type damping from the addition of the F_2 interface. This additional Gilbert damping is taken as the effect of the spin pumping.

In Fig. 1, we show a log-log plot of the contributed damping $\Delta\alpha$ as a function of the precessing bottom F_1 thickness t_{F1}. The plot shows $\Delta\alpha(t_F) = Kt^n$, with $n = -1.05 \pm 0.05$. The power law is in excellent agreement with the inverse thickness dependence of contributed damping predicted from spin pumping, $\Delta\alpha(t_F) = |\gamma|\hbar g_{\text{eff}}^{\uparrow\downarrow}/(4\pi M_s)t_F^{-1}$. The parameter $g_{\text{eff}}^{\uparrow\downarrow}$, in units of nm^{-2}, is the effective spin mixing conductance in channels per unit area. This relationship may be expressed equivalently as the product of additional Gilbert relaxation rate G and ferromagnetic layer thickness, $\Delta Gt_F = \Delta\alpha\gamma M_s t_F = \gamma^2\hbar g_{\text{eff}}^{\uparrow\downarrow}/4\pi$. Here the contribution also becomes independent of M_s. We make use of the ΔGt_F product in subsequent discussions.

The effective spin mixing conductances per interfacial area $g_{\text{eff}}^{\uparrow\downarrow}$ are listed in the second column of Table I. Spin mixing conductances for specific interfaces F_i/Cu, assumed here to be independent of growth order, can be extracted from the measurements of $g_{\text{eff}}^{\uparrow\downarrow}$. We use

$$1/g_{\text{eff}}^{\uparrow\downarrow} = 1/\tilde{g}_{F1/\text{Cu}}^{\uparrow\downarrow} + 1/\tilde{g}_{F2/\text{Cu}}^{\uparrow\downarrow}, \tag{1}$$

where $\tilde{g}_{F/N}^{-1} = g_{F/N}^{-1} - \frac{1}{2}g_{S,N}^{-1}$ is the Sharvin-corrected spin mixing conductance [30] and the Sharvin value for Cu is $g_{S,N} = 15.0\,\text{nm}^{-2}$. The effective spin mixing conductance applies to F_1 and F_2 alike. Three linear equations for g_{eff}^{-1}

TABLE I. First two columns: effective spin mixing conductances $g_{\mathrm{eff}}^{\uparrow\downarrow}$ for $F_1/N/F_2$ combinations, extracted from the data in Fig. 1; second two columns: interfacial spin mixing conductances $g_{F,N}^{\uparrow\downarrow}$ from $g_{\mathrm{eff}}^{\uparrow\downarrow}$. See text for details.

$F_1/N/F_2$	$g_{\mathrm{eff}}^{\uparrow\downarrow}(\mathrm{nm}^{-2})$	F/Cu	$g_{F/N}^{\uparrow\downarrow}(\mathrm{nm}^{-2})$
Py/Cu/Co	15.0 ± 1.5	Py	14.4 ± 1.4
Py/Cu/CoFeB	15.3 ± 1.5	CoFeB	16.0 ± 1.6
CoFeB/Cu/Co	16.8 ± 1.6	Co	15.7 ± 1.6

can be written in terms of two values of $g_{F/\mathrm{Cu}}^{-1}$ each; the system is solved for the three unknown interface values $g_{F/\mathrm{Cu}}$. The "bare" conductances $g_{F/\mathrm{Cu}}$ are tabulated in Column 4 for comparison with calculated values.

We highlight the close agreement of the three polycrystalline interfacial spin mixing conductances with each other and with theory. The three $\tilde{g}_{F/\mathrm{Cu}}$ values found from measurements of $\Delta\alpha$ all agree with the theoretical $g^{\uparrow\downarrow}$ [30] for alloyed Co/Cu(111), 14.6 nm^{-2}, within 10%. The measurements presented so far strongly support the idea that the interfacial damping in $F_i/\mathrm{Cu}/F_j$ arises from the spin pumping effect.

Because of cancellation of terms in Eq (1), spin mixing conductance at a top interface $g_{N/F_2}^{\uparrow\downarrow}$ can be extracted directly from the effective spin mixing conductance of the stack $g_{\mathrm{eff}}^{\uparrow\downarrow}$. As measured, $g_{N/F_1}^{\uparrow\downarrow}$ agrees closely with the Cu Sharvin conductance of 15.0 nm^{-2} for $F_1 = \mathrm{Co}$, Py; thus the two $g_{S,N}^{-1}/2$ terms and single $g_{N/F_1}^{\uparrow\downarrow-1}$ term cancel in Eq. (1), and we can identify $g_{\mathrm{eff}}^{\uparrow\downarrow} \simeq g_{N/F_2}^{\uparrow\downarrow}$. In the following discussion, a proportionality of Gilbert damping enhancement ΔGt_{F_1} with t_{F_2} implies a proportionality of spin current absorption near the N/F_2 interface with t_{F_2}.

We next present, in Figs. 2 and 3, measurements of the onset of spin current absorption in ultrathin layers with magnetic order. We use the thickness-dependent onset of the enhanced damping as a measure of spin current absorption. The effective spin mixing conductance $g_{\mathrm{eff}}^{\uparrow\downarrow}$ of $F_1(t_{F_1})/\mathrm{Cu}(5\ \mathrm{nm})/F_2(t_{F_2})$, $t_{F2} = 0$–15 nm is characterized through the damping enhancement $\Delta\alpha$ of F_1. In these three series, we have used the $F_1(t_{F_1}) : F_2$ combinations Co(8 nm):Py, Co(8 nm):CoFeB, and Py(10 nm):Co.

Sample data are presented in Fig. 2. We show field-swept FMR spectra at 16 GHz for Co(8 nm)/Cu(5 nm)/CoFeB(t_{CoFeB}), $t_{\mathrm{CoFeB}} = 0.5$, 3.0, and 10.0 nm. Resonances are well separated (through choice of the F_1 thickness) and the low-field Co(8 nm) resonance is monitored as a function of CoFeB coverage. The results are not sensitive to the thickness of F_1 in the range used. The higher-field resonance for the ultrathin CoFeB, which decreases in resonance field H_B as a function of t_{CoFeB} due to surface anisotropy, is not material in the data reduction.

A consequence of Eq. (1) is that the spin mixing conductance of N/F_2 affects the effective spin mixing
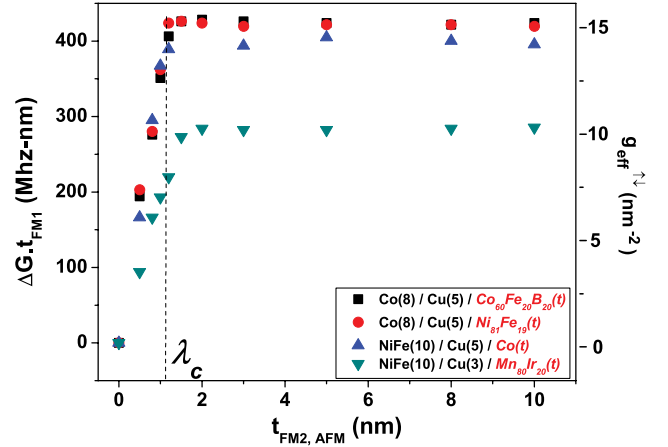

FIG. 3 (color online). Gilbert relaxation rate—F_1 layer thickness product contributed by ultrathin ferromagnets CoFeB, Py, and Co and antiferromagnet IrMn to the F_1 layer resonance in $F_1/\mathrm{Cu}(5\ \mathrm{nm})/F_2(t_{F2})$, AF2($t_{\mathrm{AF}}$). Note: Saturation level converts to $\Delta\alpha = 1.9 \times 10^{-3}$ for Co(8 nm) ($\Delta H = 0.73$ Oe/GHz), $\Delta\alpha = 2.7 \times 10^{-3}$ for Py(10 nm) ($\Delta H = 1.1$ Oe/GHz). Right axis: Conversion to effective spin mixing conductance assuming $g_L = 2.1$.

conductance for the stack, and thus the damping of F_1. In the data shown, it is possible to detect the effect of angstrom-scale coverages of CoFeB (F_2) on the low-field Co resonance (F_1). Even as the CoFeB resonance itself is at the threshold of visibility, not observed at 0.5 nm and eventually observed at 3.0 nm, the spin current absorption in CoFeB can be measured through an increase of Co linewidth of ~ 10 Oe (19%).

The frequency dependence of the Co(8 nm) linewidth as a function of CoFeB thickness (inset), plotted as $\Delta H(\omega)$, is used to separate intrinsic and extrinsic linewidth. The linear fits to $\Delta H(\omega)$ for each value of t_{CoFeB} indicate that the line broadening due to CoFeB coverage arises from both intrinsic (ω-dependent) and extrinsic (constant) components, denoted as ΔH_0. The contribution to intrinsic (Gilbert) relaxation is attributed to spin pumping.

Figure 3 presents the central result of our Letter. We plot the product ΔGt_{F1} for the three ferromagnets CoFeB, Py, Co, and for the antiferromagnet IrMn. The spin current absorption of these four layers, measured through the damping as a function of F_2 coverage, is strikingly similar. For the ferromagnets CoFeB, Py, and Co, there is a linear increase of the effective spin mixing conductance $g_{\mathrm{eff}}^{\uparrow\downarrow}$, as a function of coverage, rising to a maximum value and cutting off at a critical thickness $t = \lambda_C$, $\lambda_C = 1.2 \pm 0.1$ nm. The observed saturation values of $\Delta Gt_{F1} \simeq 410 \pm 20$ Mhz·nm for the F layers are equal within experimental error, and consistent with the values determined for the thicker trilayers in Table I. For the antiferromagnet layer IrMn, λ_C is significantly larger (1.5 nm) and the contributed relaxation rate significantly smaller,
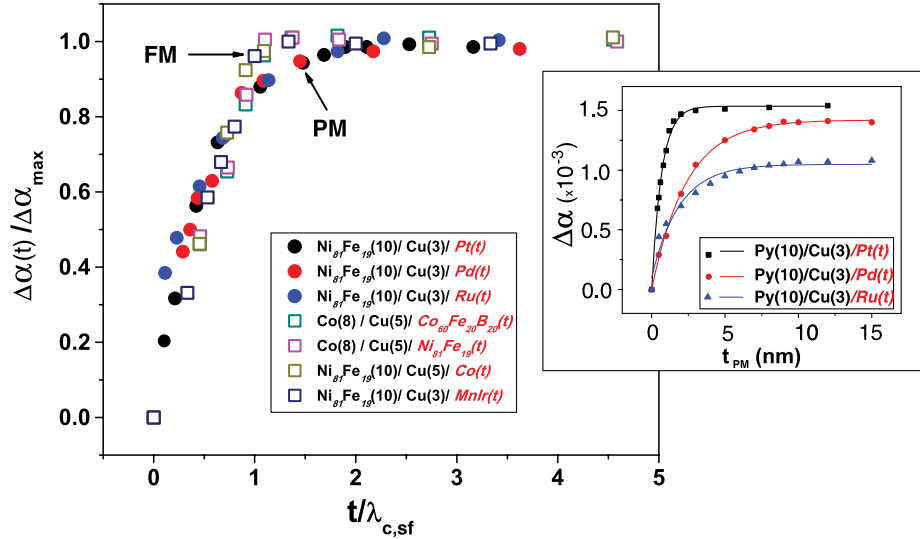
FIG. 4 (color online). Normalized plot of spin current absorption. Open symbols: Ferromagnets Co, Py, CoFeB, and antiferromagnet IrMn. Closed symbols: Paramagnetic layers Ru, Pt, and Pd. Thicknesses are normalized to the critical thickness λ_c (F, AF) or characteristic spin flip length λ_{sf} (PM); enhanced damping is normalized to its saturation value. Inset: Non-normalized data for paramagnetic layers, $\Delta\alpha(t_{PM})$; lines are exponential fits. See text for details.

$\Delta G t_{F1} \simeq 270 \pm 20$ Mhz $\cdot$ nm. There is a weaker dependence of inhomogeneous broadening ΔH_0 on overlayer thickness t_{F2}, consistent with its classification as extrinsic (defect-related, magnetostatic) in origin; see Supplemental Material [31].

The "universal" plot in Fig. 4 compares spin current absorption in the three ultrathin ferromagnets and one antiferromagnet with that previously known in paramagnets. The data in Fig. 3 are normalized in thickness to λ_C and damping size effect to $\Delta G_{max} t_{F1}$, and plotted alongside similarly prepared structures which substitute paramagnets Ru, Pd, and Pt for F_2. The paramagnetic layers show an exponential depth dependence of spin current absorption, similar to that observed by others [32,33] as $1 - \exp(-2t/\lambda_{SF})$; λ_{SF} is a characteristic length for spin relaxation in the paramagnet. Variations in the saturation value of $\Delta\alpha$ for the three PM layer coverages can be interpreted through different interface conductances $g_{Cu/PM}$ for the three Cu/PM interfaces [29]. The linear thickness dependence of spin current absorption in the magnetically ordered materials can be distinguished easily from the exponential thickness dependence in the paramagnets.

The three F layers are structurally diverse, with fcc order for Py, mixed fcc/HCP for Co, and disorder likely for CoFeB. Nevertheless, the onset of spin current absorption is identically proportional to thickness in these layers [34]. The absence of discontinuity after interface formation suggests bulk effects in the FM. A thickness proportionality of transverse spin current rotation about $\boldsymbol{M}$ in the hot-electron polarimetry measurements, both in transmission [23] and reflection [27], has been interpreted as the effect

of precession during transit, with λ_J as the thickness for a rotation of π.

For (near-Fermi surface) transport experiments, wave vectors of electrons propagating forward through the ferromagnet span 2π of the solid angle. The distribution of wave vectors with respect to the surface normal implies a distribution of transit times through F, and therefore a distribution of electron spin rotations about $\boldsymbol{M}$ while crossing F. Fermi-surface averaging thus leads to algebraic decay of the injected spin current for a given depth z: calculations predict a nonexponential convergence, as a function of t_F, of spin current absorption [24] or spin mixing conductance [7] at a $N/F(t_F)$ interface, which oscillates about the saturation value with a period of $\sim 2\lambda_J$.

We observe linear convergence, as a function of t_F, towards the saturation value of the spin mixing conductance $g^{\uparrow\downarrow}$. The result highlights the path-dependent nature of transverse spin current absorption. The net transverse spin current absorption does not result from a Poisson scattering process of uncorrelated spin-flip scatterers, but rather an angular average of continuous spin rotations for each electron wave vector in F. The absence of overshoot or oscillations would nevertheless seem to imply a mechanism which suppresses interference. Tight-binding calculations [25,26] have predicted that point defects (Fe in $Ni_{80}Fe_{20}$) are fully effective in suppressing oscillations predicted for Cu/Ni; a very similar t_F/λ_C to cutoff dependence is predicted with $\lambda_C \sim 0.7$ nm for (100) and ~ 1.1 nm for (111) structures [26]; the latter is close to our result for the FM layers. The longer value of λ_C found for the bulk antiferromagnet is consistent with weakened exchange; IrMn is nearer its Curie point of $\sim 400 \,^\circ$C.

Summary.—We have measured the thickness-dependent transverse spin current absorption in ultrathin (≤ 1 nm) polycrystalline ferromagnets using the spin pumping effect. Spin mixing conductances for thicker films >1.1 nm agree closely with theoretical predictions. Below this limit, we observe a strict proportionality in thickness which differs from both the longitudinal spin current absorption in ferromagnets and the spin current absorption in paramagnets.

---

*web54@columbia.edu

[1] M. Tsoi, A. G. M. Jansen, J. Bass, W.-C. Chiang, M. Seck, V. Tsoi, and P. Wyder, Phys. Rev. Lett. **80**, 4281 (1998).

[2] J. Katine, F. Albert, R. Buhrman, E. Meyers, and D. Ralph, Phys. Rev. Lett. **84**, 3149 (2000).

[3] J. Slonczewski, J. Magn. Magn. Mater. **159**, L1 (1996).

[4] Y. B. Bazaliy, B. Jones, and S.-C. Zhang, Phys. Rev. B **57**, R3213 (1998).

[5] S. Zhang, P. M. Levy, and A. Fert, Phys. Rev. Lett. **88**, 236601 (2002).

[6] J. Zhang, P. Levy, S. Zhang, and V. Antropov, Phys. Rev. Lett. **93**, 256602 (2004).

[7] M. Zwierzycki, Y. Tserkovnyak, P. J. Kelly, A. Brataas, and G. E. W. Bauer, Phys. Rev. B **71**, 064420 (2005).

[8] F. J. Albert, N. C. Emley, E. B. Myers, D. C. Ralph, and R. A. Buhrman, Phys. Rev. Lett. **89**, 226802 (2002).

[9] W. Chen, M. J. Rooks, N. Ruiz, J. Z. Sun, and A. D. Kent, Phys. Rev. B **74**, 144408 (2006).

[10] R. Urban, G. Woltersdorf, and B. Heinrich, Phys. Rev. Lett. **87**, 217204 (2001).

[11] B. Heinrich, Y. Tserkovnyak, G. Woltersdorf, A. Brataas, R. Urban, and G. E. W. Bauer, Phys. Rev. Lett. **90**, 187601 (2003).

[12] Y. Tserkovnyak, A. Brataas, and G. E. W. Bauer, Phys. Rev. Lett. **88**, 117601 (2002).

[13] G. Woltersdorf, O. Mosendz, B. Heinrich, and C. H. Back, Phys. Rev. Lett. **99**, 246603 (2007).

[14] S. Kiselev, J. Sankey, I. Krlvorotov, N. Emley, R. Schoelkopf, R. Buhnnan, and D. Ralph, Nature (London) **425**, 380 (2003).

[15] W. Rippard, M. Pufall, S. Kaka, S. Russek, and T. Silva, Phys. Rev. Lett. **92**, 027201 (2004).

[16] A. Brataas, Y. V. Nazarov, and G. E. W. Bauer, Phys. Rev. Lett. **84**, 2481 (2000).

[17] A. Brataas, Y. Tserkovnyak, G. E. W. Bauer, and P. J. Kelly, arXiv:1108.0385.

[18] B. Heinrich, Y. Tserkovnyak, G. Woltersdorf, A. Brataas, R. Urban, and G. Bauer, Phys. Rev. Lett. **90**, 187601 (2003).

[19] R. D. McMichael and M. D. Stiles, J. Appl. Phys. **97**, 10J901 (2005).

[20] Q. Yang, P. Holody, S.-F. Lee, L. L. Henry, R. Loloee, P. A. Schroeder, W. P. Pratt, and J. Bass, Phys. Rev. Lett. **72**, 3274 (1994).

[21] S. Steenwyk, S. Hsu, R. Loloee, J. Bass, and J. Pratt, W. P., J. Magn. Magn. Mater. **170**, L1 (1997).

[22] L. Piraux, S. Dubois, A. Fert, and L. Belliard, Eur. Phys. J. B **4**, 413 (1998).

[23] W. Weber, S. Riesen, and H. C. Siegmann, Science **291**, 1015 (2001).

[24] M. D. Stiles and A. Zangwill, Phys. Rev. B **66**, 014407 (2002).

[25] K. Carva and I. Turek, Phys. Rev. B **76**, 104409 (2007).

[26] S. Wang, Y. Xu, and K. Xia, Phys. Rev. B **77**, 184430 (2008).

[27] W. Weber, S. Riesen, C. H. Back, A. Shorikov, V. Anisimov, and H. C. Siegmann, Phys. Rev. B **66**, 100405 (2002).

[28] T. Taniguchi, S. Yakata, H. Imamura, and Y. Ando, Appl. Phys. Express **1**, 031302 (2008).

[29] A. Ghosh, J. F. Sierra, S. Auffret, U. Ebels, and W. E. Bailey, Appl. Phys. Lett. **98**, 052508 (2011).

[30] Y. Tserkovnyak, A. Brataas, G. Bauer, and B. Halperin, Rev. Mod. Phys. **77**, 1375 (2005).

[31] See Supplemental Material at http://link.aps.org/supplemental/10.1103/PhysRevLett.109.127202 for the dependence of inhomogeneous broadening ΔH_0 on t_{F2}.

[32] J. Foros, G. Woltersdorf, B. Heinrich, and A. Brataas, J. Appl. Phys. **97**, 10A714 (2005).

[33] S. Yakata, Y. Ando, T. Miyazaki, and S. Mizukami, Jpn. J. Appl. Phys. **45**, 3892 (2006).

[34] Structural issues of the ultrathin FM do not appear to be important. Our FM_2 layers are deposited on identical underlayers, (111)-textured columnar Cu, verified by TEM consistent with prior work for Ta seeding [35]. All measurements are above the threshold for ferromagnetism at 4 Å [36] and quasi-layer-by-layer grain-epitaxial growth has been seen in similarly prepared (sputtered) films in the past [37]; for Py and Co, two (111)-monolayers at 4 Å are likely to be continuous if perhaps intermixed. For the PM layers Pt and Pd, separate TEM investigations of similarly prepared ultrathin Co/Pt [38] and Pd/Cu/Pd/Co multi-layers [39] demonstrate similarly abrupt interfaces, with intermixing confined to 1–2 monolayers.

[35] S. N. R. Nakatani, K. Hoshino, and Y. Sugita, Jpn. J. Appl. Phys. **33**, 133 (1994).

[36] W. E. Bailey, S. E. Russek, X.-G. Zhang, and W. H. Butler, Phys. Rev. B **72**, 012409 (2005).

[37] W. E. Bailey, S. X. Wang, and E. Y. Tsymbal, J. Appl. Phys. **87**, 5185 (2000).

[38] G. Bertero and R. Sinclair, J. Magn. Magn. Mater. **134**, 173 (1994).

[39] M. Sakurai and T. Shinjo, J. Magn. Magn. Mater. **128**, 237 (1993).